ASYMMETRY IN ELASTIC ELECTRON SCATTERING BY GOLD ATOMS

V.I. KELEMEN, M.M. DOVHANYCH, E.YU. REMETA

Institute of Electron Physics, Nat. Acad. of Sci. of Ukraine
(21, Universytetska Str., Uzhgorod 88017, Ukraine; e-mail:
`vlad.kelemen@gmail.com; remetov@inbox.ru`*)*

PACS 34.80.Bm, 31.15.E-

The angular dependence of the spin-exchange asymmetry parameter for the elastic electron scattering by gold atoms within a collision energy range of 0.2–400 eV has been studied in the spin-polarized approximation of the optical potential (OP) method. The calculations are carried out both in the approximation of a parameter-free real OP part and with the use of a complex-valued OP to take absorption effects into account. Two types of the absorption potential were used as the imaginary part of OP. The systematic calculations of the asymmetry were carried out with the use of an empiric absorption potential. An energy-dependent parameter in this potential was determined in the approximation of quasifree electron scattering with the use of a non-empiric absorption potential. The angular dependence of the asymmetry parameter in a wide energy range is shown to be governed by the spin dependences of both exchange and polarization interactions between an electron and an atom. A large influence of absorption effects on the asymmetry parameter behavior is revealed. It is shown that the asymmetry parameter at small scattering angles depends on the choice of the absorption potential even at energies of several hundred eV.

1. Introduction

For the description of the process of elastic potential electron scattering by a multielectron atom to be consistent, model interaction potentials are to be determined in the framework of one-type approximations. Theoretical approximations that are used for finding those potentials must originate from the peculiarities of the electron structure of a target and take them into account. Atomic systems with a single half-filled electron subshell were described in the spin-polarized approximation [1,2], i.e. with regard for the spin polarization of the subshell. According to the Hund rule [1], the ground state of such systems has a maximal spin which is determined by the total spin of electrons in the half-filled subshell. Therefore, the whole electron shell of an atom is divided into two filled spin subshells.

A gold atom has the half-filled valence $6s^1$ subshell and precedes a mercury atom in the Periodic table. For the latter, there are a lot of experimental data in the literature concerning the process of elastic electron scattering. These are not only various scattering cross-sections (see, e.g., work [3] and the references therein), but also such precise characteristics as the spin polarization parameters of a scattered electron (see, e.g., work [4] and the references therein).

In contrast to mercury atoms, there are few experimental data for the elastic scattering of electrons by gold atoms. For instance, in work [5], the differential cross-sections (DCSs) of electron elastic scattering by gold atoms were measured for only four values of incident electron energy; namely, 30, 50, 100, and 200 eV. In works [6, 7], the ionization cross-sections of gold atoms were measured.

In this work, the angular dependence of the spin-exchange asymmetry parameter has been calculated in a wide energy interval from 0.2 to 400 eV. It is the first information concerning such a characteristic of the elastic electron scattering that is rather sensitive to the choice of both experimental techniques and theoretical approximations.

To find the electron orbitals, the total and subshell electron densities, and the scattering potentials, we used the local spin density (LSD) approximation of the density functional theory (DFT) [2]. In this approximation, the whole electron shell of Au atom with a spin of 1/2 is divided into two filled spin subshells, with 40 spin-up (sp $=\uparrow$) and 39 spin-down (sp $=\downarrow$) electrons, respectively. As a result of atomic calculations for those subshells, we have two electron spin densities $\rho_\uparrow(r)$ and $\rho_\downarrow(r)$ which are denoted below as $\rho_{\rm sp}(r)$. The total electron density of the atom is $\rho(r)=\rho_\uparrow(r)+\rho_\downarrow(r)$.

In the case of an incident electron with a fixed spin direction and a spin-polarized atom, the exchange interaction is possible only with the electrons of the corresponding atomic spin subshell. Hence, the scattering of electrons by a gold atom can be considered in the cases where the directions of the spins of the incident electron and the atom are either parallel ($\uparrow\uparrow$) or antiparallel ($\downarrow\uparrow$).

In this work, the spin dependence is also considered in the polarization interaction between the incident electron and the atom. For this purpose, we used an approximation, in which the polarization interaction in an internal atomic region is governed by the correlation interaction between the incident electron and electrons of the target (as was done, e.g., in works [8, 9]). In the DFT, this interaction is described by a correlation functional which is determined in the LSD approximation for a nonuniform spin-polarized electron gas by the correlation energy density $\varepsilon_c[\rho_\uparrow(r),\rho_\downarrow(r)]$. As was done in our work (see work [10] and the references therein), the spin-dependent polarization potentials are determined in what follows.

At energies higher than the first excitation threshold of target atoms, the elastic scattering of electrons is accompanied by the inelastic one. To take this energy absorption into account, a certain absorption potential is used as the imaginary part of OP. In this work, similarly to what was done in work [10], the asymmetry was calculated with the use of two types of absorption potential: an empiric potential proposed in [11, 12] and a nonempiric absorption potential in the quasifree electron scattering approximation [13]. Both potentials depend on the exchange and polarization ones. Accordingly, the description of the absorption in the spin-polarized approximation depends on the orientation of the incident electron spin. As a result of calculations with two different OPs, we obtain the different cross-sections for parallel and antiparallel scattering. As a consequence, we obtain a function that describes the spin exchange asymmetry of scattering.

In the series of previous researches dealing with the electron scattering by atoms with a single unfilled shell (see, e.g., works [14, 15]), the correlation-polarization potentials obtained in works [8, 9] for the case $\rho_\uparrow(r)=\rho_\downarrow(r)$ were used to take the polarization interaction into account.

Hence, to demonstrate that the spin dependence of the polarization interaction has to be taken into consideration, we also calculated the asymmetry parameter with the help of correlation-polarization potential similar to that used in work [9].

2. Theoretical Method

To study the electron scattering by a gold atom in two cases – with parallel ($\lambda=\uparrow\uparrow$) and antiparallel ($\lambda=\downarrow\uparrow$) spin orientations – we used OP in the local spin-polarized approximation (LSPA)

$$V^\lambda_{\rm opt}(r,E)=V^\lambda_R(r,E)+iV^\lambda_a(r,E). \qquad (1)$$

Its real part, $V^\lambda_R(r,E)$, is a sum of the static, $V_{\rm st}(r)$, exchange, $V^\lambda_{\rm ex}(r,E)$, polarization, $V^\lambda_{\rm pol}(r)$, and spin-orbit interaction, $V^\pm_{\rm so}(r)$, potentials:

$$V^\lambda_R(r,E)=V_{\rm st}(r)+V^\lambda_{\rm ex}(r,E)+V^\lambda_{\rm pol}(r)+V^\pm_{\rm so}(r). \qquad (2)$$

In Eq. (2), the notation ± corresponds to the magnitude of the total angular momentum of the electron $j=\ell\pm1/2$, ℓ is the orbital momentum of the electron, E is the energy, and $k=(2E)^{1/2}$ is the momentum of the incident electron (hereafter, we use the atomic system of units with $e=m_e=\hbar=1$). The imaginary part $V^\lambda_a(r,E)$ in Eq. (1) is an absorption potential.

Analogously to our previous works (see, e.g., works [15–17] and the references therein), calculations for the complex-valued potential (1) will be named to as a $V_{\rm opt}$-approximation, and calculations for the real potential (2) as a $V_{\rm R}$-one.

The static potential $V_{\rm st}(r)$, the electron orbital $\varphi_{6s}(r)$, and the densities $\rho(r)$ and $\rho_{\rm sp}(r)$ were found numerically in a self-consistent atomic calculation in the frameworks of the scalar-relativistic and LSD approximations of the DFT with the exclusion of the electron self-action energy (see, e.g., Section 2.2 in work [18] and the references therein). Those quantities were approximated by analytical expressions taken from work [19] (see (A.1) and (A.2), as well as the corresponding parameters, in Appendix A). The spin-orbit interaction potential $V^\pm_{\rm so}(r)$ (it is proportional to the derivative ${\rm d}V_{\rm st}/{\rm d}r$) looks like Eq. (6) in work [20] (see also the references therein).

To find the exchange interaction potentials, we used the free electron gas approximation (see, e.g., expression (2) in work [21] and the references therein). In the LSPA, there are two spin potentials $V^\lambda_{\rm ex}(r,E)$: $V^{\uparrow\uparrow}_{\rm ex}$ with $k^\uparrow_{\rm F}$, and $V^{\downarrow\uparrow}_{\rm ex}$ with $k^\downarrow_{\rm F}$. The Fermi spin momenta are $k^{\rm sp}_{\rm F}(r)=[6\pi^2\rho_{\rm sp}(r)]^{1/3}$. The ionization potential of a gold atom $I=9.2256$ eV, which is needed for the calculation of $V^\lambda_{\rm ex}$, was taken from work [22].

The polarization potential, similarly to works [8, 9], consists of two parts separately determined at short (SR) and long (LR) distances:

$$V_{pol}^{\lambda}(r) = \begin{cases} Vp_{\lambda}^{\mathrm{SR}}(r), & r \le r_c^{\lambda} \\ Vp^{\mathrm{LR}}(r), & r > r_c^{\lambda}. \end{cases} \quad (3)$$

In the internal atomic region, $V_{\mathrm{pol}}^{\lambda}$ is governed by the correlation interaction between the incident electron and target electrons. In the LSD approximation of DFT, the functional of this interaction is

$$E_c^{\mathrm{LSD}}[\rho_{\uparrow}, \rho_{\downarrow}] = \int d\mathbf{r} \rho(\mathbf{r}) \varepsilon_c[\rho_{\uparrow}(\mathbf{r}), \rho_{\downarrow}(\mathbf{r})]. \quad (4)$$

The energy density $\varepsilon_c[\rho_{\uparrow}(r), \rho_{\downarrow}(r)] \equiv \varepsilon_c[r_s(r), \zeta(r)]$ is determined by the spin polarization function $\zeta(r) = [\rho_{\uparrow}(r) - \rho_{\downarrow}(r)]/\rho(r)$ and the function $r_s(r) = \{3/[4\pi\rho(r)]\}^{1/3}$. It is calculated by formulas (B.1)–(B.4) in Appendix B. Hence, at distances $r \le r_c^{\lambda}$, the polarization potential obtained by varying expression (4) is [10]

$$Vp_{\lambda}^{\mathrm{SR}}(r) = \varepsilon_c(r_s, \zeta) - \frac{r_s}{3}\frac{\partial \varepsilon_c}{\partial r_s} \pm (1 \mp \zeta)\frac{\partial \varepsilon_c}{\partial \zeta}. \quad (5)$$

In Eq. (5), the upper signs + and − correspond to the case $\lambda = \uparrow\uparrow$, whereas the lower signs − and + to the case $\lambda = \downarrow\uparrow$. The derivatives $\partial\varepsilon_c/\partial r_s$ and $\partial\varepsilon_c/\partial\zeta$ in Eq. (5) are defined by formulas (B.5)–(B.7) in Appendix B. At distances $r > r_c^{\lambda}$, the polarization potential has the well-known asymptotic behavior $Vp^{\mathrm{LR}}(r) = -\alpha_d(0)/2r^4$, where $\alpha_d(0)$ is the static dipole polarizability (see, e.g., Eq. (12) in work [8]). Two parts of the polarization potential, $Vp_{\lambda}^{\mathrm{SR}}(r)$ and $Vp^{\mathrm{LR}}(r)$, intersect each other for the first time at the points $r_c^{\uparrow\uparrow} = 9.544a_0$ for the case of parallel ($\lambda = \uparrow\uparrow$) and $r_c^{\downarrow\uparrow} = 11.6a_0$ for the case of antiparallel ($\lambda = \downarrow\uparrow$) scattering. The polarizability of a gold atom $\alpha_d(0) = 33.3a_0^3$ was calculated in the local approximation of time-dependent DFT [23] with a relativistic effective local potential.

At collision energies higher than the first inelastic threshold energy, $\Delta = 1.1358$ eV [22], the calculations were carried out in the approximation of a complex-valued potential $V_{\mathrm{opt}}^{\lambda}(r, E)$ (Eq. (1)), the V_{opt} one, with regard for absorption effects in the scattering. Absorption potentials of two types were used as the imaginary part $V_a^{\lambda}(r, E)$. The asymmetry parameter was calculated with the use of an empiric potential proposed in [11,12] and modified in [13] (see expression (17)). In the LSPA, this absorption potential takes the form

$$VaMc_{\lambda}(r, E) = -W_{\lambda}(E) r^2 \rho_{6s}(r)/[T_{\mathrm{loc}}^{\lambda}(r, E)]^2. \quad (6)$$

Here, $W_{\lambda}(E)$ is a phenomenological parameter, $\rho_{6s}(r)$ is the electron density of the valence $6s$-subshell of a gold atom (see Eq. (C.1) in Appendix C), and the local kinetic energy is $T_{\mathrm{loc}}^{\lambda} = E - V_{\mathrm{st}} - V_{\mathrm{ex}}^{\lambda} - V_{\mathrm{pol}}^{\lambda}$.

To obtain the energy dependence of the parameter $W(E)$ in potentials of type (6), we can use the experimental integral cross-sections of inelastic electron scattering by atoms (as it was made by us for indium atoms in [15]). Since there are few data in the literature on such cross-sections for gold atoms, in this work, as well as in work [17], we used the theoretical integral cross-sections of inelastic scattering $\sigma_{\mathrm{abs}}^{\lambda}(E)$. These cross-sections were calculated using modified version 2 ($Vaf2m(r, E)$) [24] of a non-empiric absorption potential in the quasifree electron scattering [13]. In the spin-polarized approximation, this potential is determined by the potentials $V_{\mathrm{ex}}^{\lambda}(r, E)$ and $V_{\mathrm{pol}}^{\lambda}(r)$. It gives rise to two spin-dependent absorption potentials $Vaf2m_{\lambda}(r, E)$.

The modification of version 2 of the potential from work [13] in the LSPA consists in the following. First, the local velocity of an incident electron is $\nu_{\mathrm{loc}}^{\lambda} = [2(E - V_{\mathrm{st}} - V_{\mathrm{ex}}^{\lambda} - V_{\mathrm{pol}}^{\lambda})]^{1/2}$. Second, the parameters $\alpha_{\lambda}(r, E)$ and $\beta_{\lambda}(r, E)$ are $\alpha_{\lambda} = k_{\mathrm{F}}^2 + \Delta - 2(V_{\mathrm{st}} + V_{\mathrm{ex}}^{\lambda} + V_{\mathrm{pol}}^{\lambda})$ and $\beta_{\lambda} = \alpha_{\lambda}$ (cf. expressions (21a) and (21b) from work [13]). In this case, the Fermi local momentum $k_{\mathrm{F}}(r) = [3\pi^2\rho(r)]^{1/3}$ is determined by the total density of atomic electrons $\rho(r)$.

There is no doubt that, using the absorption potential $Vaf2m_{\lambda}$, not only the cross-sections $\sigma_{\mathrm{abs}}^{\lambda}(E)$, but also the DCSs and the asymmetry parameter can be calculated. However, as was shown by us in work [17], the angular dependence of the DCS of elastic electron scattering by ytterbium atoms at $E < 40$ eV, which was calculated with the use of an absorption potential of type (6), agreed better with experiment, than it was in the case of the non-empiric potential. Concerning the angular dependence of the asymmetry parameter, it is even more sensitive to the choice of that or another absorption potential (see below).

In addition, in this work, we determined the contribution of the potentials $V_{\mathrm{ex}}^{\lambda}(r, E)$ and $V_{\mathrm{pol}}^{\lambda}(r)$ to the asymmetry. For this purpose, in the framework of the V_{R}-approximation and in addition to calculations with potential (2), we also examined the angular dependence of the asymmetry parameter by using the scattering potential

$$VR2_{\lambda}(r, E) = V_{\mathrm{st}}(r) + V_{\mathrm{ex}}^{\lambda}(r, E) + V_{\mathrm{pol}}(r) + V_{\mathrm{so}}^{\pm}(r). \quad (7)$$

Here, at small distances $r \le r_c$ and at $\zeta(r) = 0$, i.e. when $\rho_{\uparrow}(r) = \rho_{\downarrow}(r)$, the polarization potential $V_{\mathrm{pol}}(r)$ is equal to the correlation-polarization one $Vp^{\mathrm{SR}}(r)$ (5). It corresponds to the local spin-unpolarized approximation in the scattering. The two parts of the potential $V_{\rm pol}(r)$– namely, $Vp^{\rm SR}(r)$ and $Vp^{\rm LR}(r)$ – intersect at the point $r_c = 5.346a_0$ for the first time. Hence, when calculating with $VR2_\lambda(r,E)$, we neglect the spin dependence of the polarization interaction. As is demonstrated below, while calculating the asymmetry parameter for the electron scattering by an atom possessing a half-filled valence subshell, it is not enough to take the spin dependence of the exchange interaction only into consideration.

Calculations with the potentials $V^\lambda_{\rm opt}(r,E)$ (1) give rise to four collections of partial complex phase shifts $\delta^{\lambda,\pm}_\ell(E) = \varepsilon^{\lambda,\pm}_\ell(E)+i\mu^{\lambda,\pm}_\ell(E)$. Accordingly, calculations with potentials (2) and (7) bring about four collections of real-valued phase shifts. For phase calculations, as was done in our previous works [15–17, 20, 21, 24], we applied the phase function method [25, 26]. The routine of a numerical solution of the phase equations was reported in works [15, 17, 20]. Knowing the phase shifts $\delta^{\lambda,\pm}_\ell$, we can determine the “direct” scattering amplitudes

$$f^\lambda(E,\theta) = \frac{1}{2ik}\sum_{\ell=0}^{\infty}\{(\ell+1)[\exp(2i\delta^{\lambda,+}_\ell)-1]+$$

$$+\ \ell[\exp(2i\delta^{\lambda,-}_\ell)-1]\}P_\ell(\cos\theta) \qquad (8)$$

and the “spin-flip” scattering amplitudes

$$g^\lambda(E,\theta) = \frac{1}{2ik}\sum_{\ell=0}^{\infty}\Big[\exp(2i\delta^{\lambda,-}_\ell)-$$

$$-\exp(2i\delta^{\lambda,+}_\ell)\Big]P^1_\ell(\cos\theta), \qquad (9)$$

where θ is the scattering angle, $P_\ell(\cos\theta)$ are Legendre polynomials, and $P^1_\ell(\cos\theta)$ are associated Legendre functions of the first kind.

The spin DCSs of parallel, $d\sigma^{\uparrow\uparrow}/d\theta$, and antiparallel, $d\sigma^{\downarrow\uparrow}/d\theta$, elastic scattering are determined by those amplitudes by the formula

$$\frac{d\sigma^\lambda(E,\theta)}{d\theta} = |f^\lambda(E,\theta)|^2 + |g^\lambda(E,\theta)|^2. \qquad (10)$$

When a completely polarized electron beam is scattered by a polarized atom, the parameter of spin exchange asymmetry $A(E,\theta)$ is determined by the expression [27]

$$A(E,\theta) = (d\sigma^{\downarrow\uparrow}/d\theta - d\sigma^{\uparrow\uparrow}/d\theta)/(d\sigma^{\downarrow\uparrow}/d\theta + d\sigma^{\uparrow\uparrow}/d\theta). \qquad (11)$$

Note that, in the case of the electron scattering by atoms with a half-filled s-subshell, the cross-sections $d\sigma^{\uparrow\uparrow}/d\theta$ and $d\sigma^{\downarrow\uparrow}/d\theta$ are related to the known singlet (S) and triplet (T) cross-sections:

$$\frac{d\sigma^{\rm S}}{d\theta} = 2\frac{d\sigma^{\downarrow\uparrow}}{d\theta} - \frac{d\sigma^{\uparrow\uparrow}}{d\theta}, \qquad \frac{d\sigma^{\rm T}}{d\theta} = \frac{d\sigma^{\uparrow\uparrow}}{d\theta}. \qquad (12)$$

Then, the averaged differential cross-section of elastic scattering can be found by the formula

$$\frac{d\sigma}{d\theta} = \frac{1}{2}\left(\frac{d\sigma^{\uparrow\uparrow}}{d\theta} + \frac{d\sigma^{\downarrow\uparrow}}{d\theta}\right). \qquad (13)$$

Accordingly, asymmetry (11) is determined in terms of the singlet and triplet cross-sections as

$$A(E,\theta) = (d\sigma^{\rm S}/d\theta - d\sigma^{\rm T}/d\theta)/(d\sigma^{\rm S}/d\theta + 3d\sigma^{\rm T}/d\theta).$$

The cross-section of inelastic scattering $\sigma^\lambda_{\rm abs}(E)$, which, in general, describes the processes of atomic excitation and ionization from the ground state, is calculated by the formula

$$\sigma^\lambda_{\rm abs}(E) = \frac{\pi}{2E}\sum_\ell\{(\ell+1)[1-\exp(-4\mu^{\lambda,+}_\ell)]+$$

$$+\ell[1-\exp(-4\mu^{\lambda,-}_\ell)]\}. \qquad (14)$$

3. Discussion of Results

The angular dependence of the asymmetry parameter $A(E,\theta)$ (11) at the elastic scattering of electrons by gold atoms was calculated for the energy of an incident electron ranging from 0.2 to 400 eV. The calculations of $A(E,\theta)$ taking no absorption effects into account, i.e. in the $V_{\rm R}$-approximation, were carried out for both the potential $V^\lambda_R(r,E)$ (2) and the potential $VR2_\lambda(r,E)$ (7), in which the spin dependence was made taken only in the exchange interaction $V^\lambda_{ex}(r,E)$ into account. Calculations with absorption effects, i.e. the $V_{\rm opt}$-approximation (1), were carried out with the absorption potential $VaMc_\lambda(r,E)$ (6). As was marked above, for the calculations of the energy dependence of the parameters $W_\lambda(E)$ for potential (6), we used here the inelastic cross-section $\sigma^\lambda_{\rm abs}(E)$ (14) calculated with the use of the nonempiric absorption potential $Vaf2m_\lambda(r,E)$. The corresponding values obtained for the parameters $W_\lambda(E)$ are quoted in Table 1.

In Fig. 1, the energy dependences of the cross-sections $\sigma^{\uparrow\uparrow}_{\rm abs}$ and $\sigma^{\downarrow\uparrow}_{\rm abs}$, as well as the experimental ionization cross-sections taken from works [6, 28], are depicted.

Parameters $W_\lambda(E)$ (in a.u.) for the absorption potential $VaMc_\lambda$ (6)

E (eV)	5	10	15	20	40	60	80	100	200	300	400
$W_{\uparrow\uparrow}$	0.1803	1.028	2.392	4.179	14.864	30.993	51.968	77.004	252.04	495.70	792.87
$W_{\downarrow\uparrow}$	0.1417	0.882	2.118	3.7343	13.225	27.328	45.748	67.70	221.29	435.76	698.10

One can see that the cross-section $\sigma_{\text{abs}}^{\uparrow\uparrow}$ exceeds $\sigma_{\text{abs}}^{\downarrow\uparrow}$ within the whole energy interval; in particular, it is 1.1 times larger at the maximum located at 10 eV. Since, the literature data on experimental inelastic scattering cross-sections present only the ionization cross-sections $\sigma_{\text{ion}}(E)$, just these cross-sections are demonstrated in Fig. 1. The cross-section of complete ionization σ_{ion} has a maximum at 100 eV according to the results of work [6], which does not agree with the results of other works. For instance, in experimental work [7], the cross-section maximum was obtained at 70 eV for the complete ionization and at 50 eV for the single ionization. A semiempiric calculation carried out in work [29] gave a maximal value of 5.0×10^{-20} m^2 for the cross-section of Au atom single ionization at 70 eV. In work [6], the ratio $\sigma_{\text{ion}}(\text{Au})/\sigma_{\text{ion}}(\text{Cu}) = 2.0 \pm 0.2$ between the ionization cross-sections for gold and copper atoms at energies from 50 to 180 eV was found. In work [28], the single ionization cross-section for copper atoms was measured. The doubled values of this cross-section within the energy interval 50–180 eV are presented in Fig. 1 as the data taken from work [28]. Note that, in the cited work, the cross-section $\sigma_{\text{ion}}(\text{Cu})$ had a maximum at 34 eV. Figure 1 testifies that the results of our calculations agree better with the data of work [28] than with those of work [6].

The angular dependence of the asymmetry parameter in the energy range 0.2–3 eV is characterized by a smooth behavior. By the absolute value, the function $A(E,\theta)$ does not exceed 0.2. Starting from 3 eV, the shape of this function is similar to results of the corresponding calculation of the asymmetry parameter at 5 eV (see Fig. 2,*a*).

In Fig. 2, the angular dependences of the asymmetry parameter calculated in three approximations are exhibited. The first approximation takes the absorption effects into account and uses the complex potential $V_{opt}^{\lambda}(r,E)$ (1). Two other approximations do not consider the absorption effects and use either of the potentials $V_R^{\lambda}(r,E)$ (2) or $VR2_\lambda(r,E)$ (7). One should bear in mind that, in calculations where $VR2_\lambda$ is used, the spin dependence of the correlation-polarization interaction is neglected.

As is evident from Fig. 2,*a*, the angular dependence $A(E,\theta)$ calculated for 5 eV with regard for the absorption effects is mainly in agreement with the results of V_R^{λ}-calculations. Only at angles larger than 120°, the asymmetry values differ not only by the magnitude, but also by the sign. On the contrary, the results of $VR2_\lambda$-calculations differ drastically from those with V_R^{λ}. In particular, the former includes two minima at 53 and 116° and a maximum at 99°. At the same time, calculations with V_R^{λ}, as well as with V_{opt}^{λ}, bring about only one minimum at about 98°. Note that, for energies lower than 5 eV, the difference between the behavior of the angular dependences of the asymmetry parameter obtained with $VR2_\lambda$ and V_R^{λ} potentials increases, when approaching the elastic process threshold.

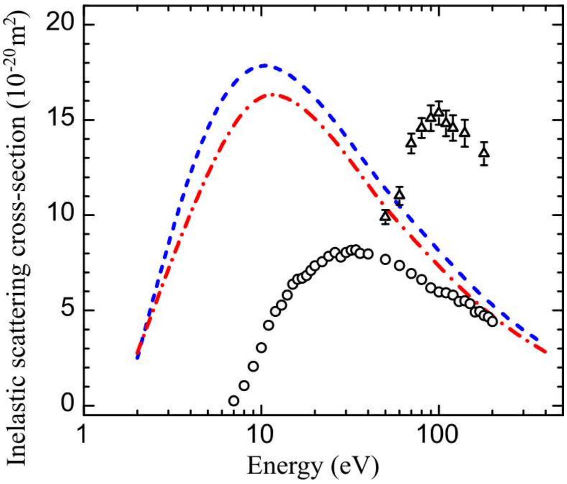

Fig. 1. (color on-line) Energy dependences of the inelastic electron scattering cross-sections $\sigma_{\text{abs}}^{\lambda}(E)$ (in units of 10^{-20} m^2) by gold atoms calculated in the V_{opt}-approximation (1) with a modified absorption potential $Vaf2m_\lambda(r,E)$ taken from work [13]: $\sigma_{\text{abs}}^{\uparrow\uparrow}$ (dashed curve), $\sigma_{\text{abs}}^{\downarrow\uparrow}$ (dash-dotted curve), experimental cross-sections of complete ionization of Au atom (triangles, taken from work [6]), doubled cross-sections of single ionization of copper atoms (circles, taken from work [28])

For 10 eV (see Fig. 2,*b*), the result of calculations with V_{opt}^{λ} (1) has a more structured angular dependence in comparison with the previous plot; namely, there are three minima and two maxima instead of one minimum. The result of calculations with V_R^{λ} (2) and neglecting absorption agrees, in general, at intermediate and high scattering angles with the result of V_{opt}^{λ}-calculations: at angles larger than 40°, the numbers of minima and maxima are the same, and they have almost identical angular positions. Only at low angles, smaller than 40°,

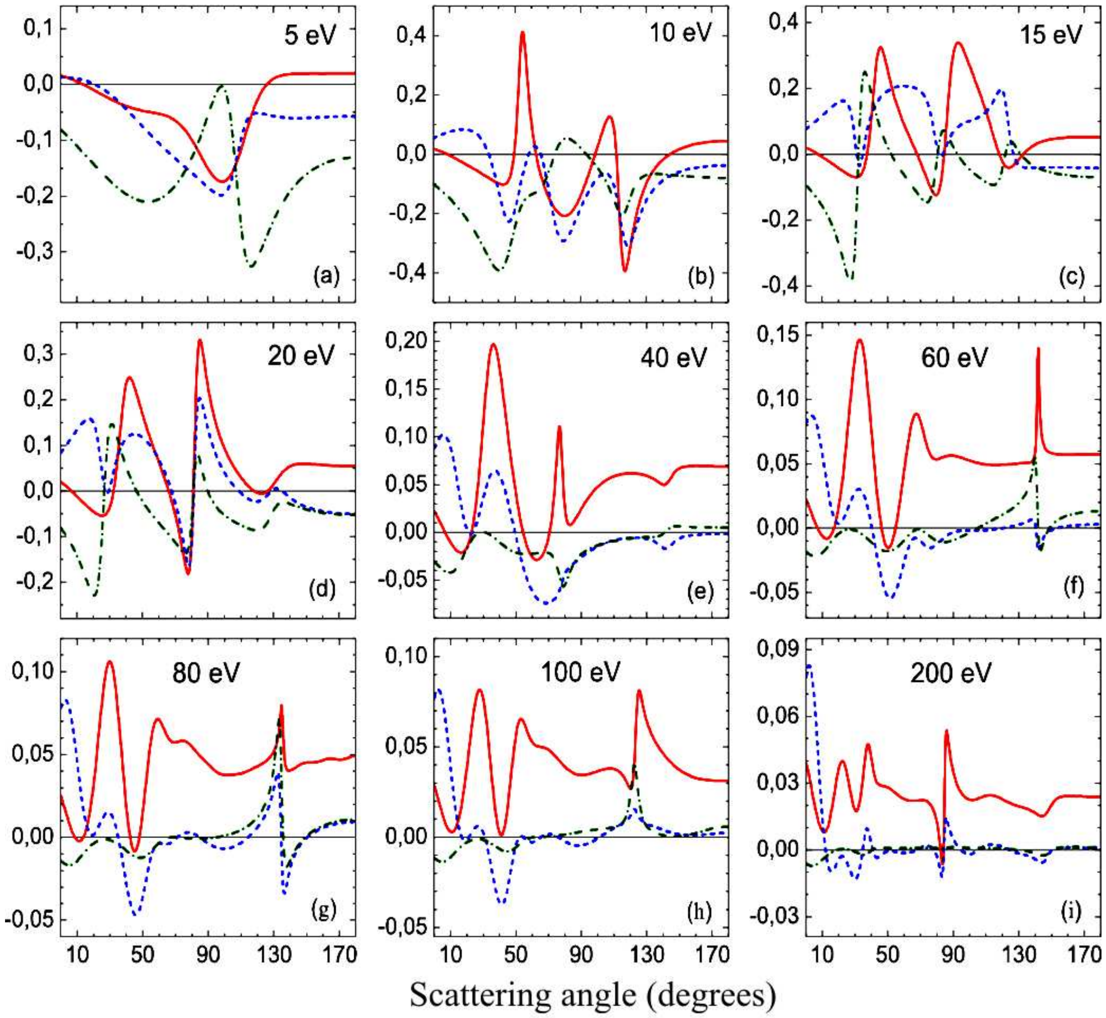

Fig. 2. (color on-line) Angular dependences of the asymmetry parameter $A(E,\theta)$ for the elastic electron scattering by gold atoms at energies of 5, 10, 15, 20, 40, 60, 80, 100, and 200 eV (panels *a* to *i*): $V_{\rm opt}$-calculation (formula (1)) with the absorption potential $VaMc_\lambda(r,E)$ (formula (6)) (solid curve); $V_{\rm R}$-calculations taking no absorption effects into account and with the potentials $V_R^\lambda(r,E)$ (formula (2), dashed curve) and $VR2_\lambda(r,E)$ (formula (7), dash-dotted curve)

these calculations differ substantially from one another. The result of calculations with $VR2_\lambda$ in the angular interval 0–100° differs considerably from that of the V_R^λ-calculation. In particular, there is no maximum at 60°, and there is a maximum at 80° rather than a minimum, which was obtained in the $VR2_\lambda$-based calculation.

For 15 eV (see Fig. 2,*c*), in contrast to the previous plot, the results of $V_{\rm opt}^\lambda$- and V_R^λ-calculations are different in the whole angle interval. In its turn, the result of $VR2_\lambda$-based calculations differs even more both qualitatively and quantitatively from that of calculations with V_R^λ in the angle interval $0-130°$.

For 20 eV (see Fig. 2,*d*), the results of calculations with $V_{\rm opt}^\lambda$ and V_R^λ are in a qualitative and, at some angles, even quantitative agreement in the angle interval $30-130°$. In contrast to calculations with the potential $V_{\rm opt}^\lambda$, calculations with V_R^λ for angles less than 30° gave a positive asymmetry maximum at 20° and negative values of the parameter $A(E,\theta)$ at angles larger than 130°. At angles larger than 70°, the results of two $V_{\rm R}$-calculations with $VR2_\lambda$ and V_R^λ are in a qualitative agreement. At smaller angles, the $VR2_\lambda$-based calculation gave the asymmetry maximum at 32° and a minimum at 21°, instead of two maxima and a minimum at 28° obtained in calculations with V_R^λ.

For 40 eV (Fig. 2,*e*), in contrast to the results of $V_{\rm R}$-calculations, the account of the absorption effects calculated with $V_{\rm opt}^\lambda$ gave rise to a sharp maximum of the asymmetry parameter at 76.5°. In general, the results of calculations with V_{opt}^{λ} and V_R^{λ} are in a qualitative agreement almost in the whole angle interval. The results of calculations carried out neglecting the spin dependence of the correlation-polarization interaction are still substantially different at small angles less than 80° from those obtained in the V_R^{λ}-calculation. At larger angles, the difference between the results of those calculations reveal itself only in the range $130 - 150°$; in particular, these are positive asymmetry values and the absence of a negative minimum in the results of calculations with $VR2_{\lambda}$.

As is seen from Fig. 2,*f* plotted for 60 eV, the results of calculations with V_{opt}^{λ} and V_R^{λ} qualitatively agree almost in the whole angle interval, as it was at the previous energy value. The main difference in this case takes place at an angle of 142°, where the account of the absorption effects resulted in the appearance of a sharp peak in the asymmetry parameter. In addition, the function $A(E,\theta)$ in the V_{opt} approximation is positive almost in the whole angle interval, being larger by the absolute value that the corresponding results obtained in calculations with V_R^{λ}. The angular dependences of the asymmetry parameter obtained in calculations with $VR2_{\lambda}$ and V_R^{λ} at angles $140 - 143°$ have identical behavior of the maximum–minimum type. However, the $VR2_{\lambda}$-calculations bring about an $A(E,\theta)$-maximum that is about eight times larger than that obtained in more precise calculations with V_R^{λ}. This gives grounds for admitting a certain mutual compensation between the spin exchange and spin polarization interactions. For angles less than 105°, the asymmetry parameter in the $VR2_{\lambda}$-based calculation is negative; it has three local minima and two maxima. For the same angles, the V_R^{λ}-based calculation gave negative values only in the range $40 - 105°$ and positive ones at $\theta < 40°$. At last, at angles close to zero, the asymmetry parameter in this calculation is almost four times larger than that in the calculation with V_{opt}^{λ}.

As is seen from Fig. 2,*g*, an increase of the incident electron energy by 20 eV did not result, in comparison with the previous plot, to a considerable variation of the angular dependence of the asymmetry parameter in all three approximations. The largest difference between the results of V_{opt}-calculations is observed for a maximum at 134.5° obtained for 80 eV, which is almost half as large as a maximum at 142° obtained for 60 eV. For the same angles in the V_R^{λ}-calculation, the difference between the extrema of the function $A(E,\theta)$ is much larger than that for 60 eV. The maximum value of the asymmetry parameter at 133° in the $VR2_{\lambda}$-calculation is almost the same as obtained in the calculation with V_{opt}^{λ}.

Starting from 10 eV, the maximal values of $A(E,\theta)$ in V_{opt}-calculations decrease with the energy. At $E \geq 40$ eV, it mainly concerns a low-angle maximum at about 30°. The magnitude of the asymmetry parameter in this maximum was equal to 0.106 for 80 eV (Fig. 2,*g*), 0.082 for 100 eV (Fig. 2,*h*), and only 0.04 for 200 eV (Fig. 2,*i*) at 22°. Concerning the high-angle maximum, its position by the results of calculations with V_{opt}^{λ} moves toward smaller angles as the energy grows. For instance, the maximum is located at 142° for 60 eV, and at 86° for 200 eV. In addition, the behavior of the function $A(E,\theta)$ in a vicinity of this maximum changes as the energy increases: from a sharp maximum obtained for 60 eV to an angular dependence of the minimum–maximum type obtained for 200 eV.

In contrast to 80 eV, the absolute values of the asymmetry parameter obtained for 100 and 200 eV in V_{R}-calculations carried out for angles larger than 12° are considerably smaller than the corresponding value calculated taking the absorption effects into account. The minimum at 42° and the maximum at 122° obtained for 100 eV (Fig. 2,*h*) in the V_R^{λ}- and $VR2_{\lambda}$-based calculations, respectively, are exceptions.

At last, consider the sensitivity of the angular dependences of DCS and, hence, the asymmetry parameter to the choice of the absorption potential $V_a^{\lambda}(r,E)$ in the V_{opt}-approximation (1). In Fig. 3, the results of calculations of average DCSs (13) and $A(E,\theta)$ in the V_{R}-approximation with V_R^{λ} (2), as well as the results of two V_{opt}-calculations with the use of the absorption potentials $VaMc_{\lambda}$ (6) and $Vaf2m_{\lambda}$, are exhibited. The figure demonstrates that, for an energy of 400 eV, the results of all three DCS calculations are almost coincide with each other. On the contrary, the angular dependences of the asymmetry parameter calculated in the V_{R} and V_{opt} approximations are different. In their turn, those dependences obtained in V_{opt}-calculations with $VaMc_{\lambda}$ and $Vaf2m_{\lambda}$ differ quantitatively only at angles of 10–50°. One can note the absence of a maximum at 39° in the $Vaf2m_{\lambda}$-calculation and the presence of deeper minima at 33 and 22°, where the function $A(E,\theta)$ is negative.

4. Conclusions

The angular dependence of the spin exchange asymmetry parameter $A(E,\theta)$ of the elastic electron scattering by gold atoms has been calculated and analyzed for the first time in a wide interval of collision energies from 0.2 to

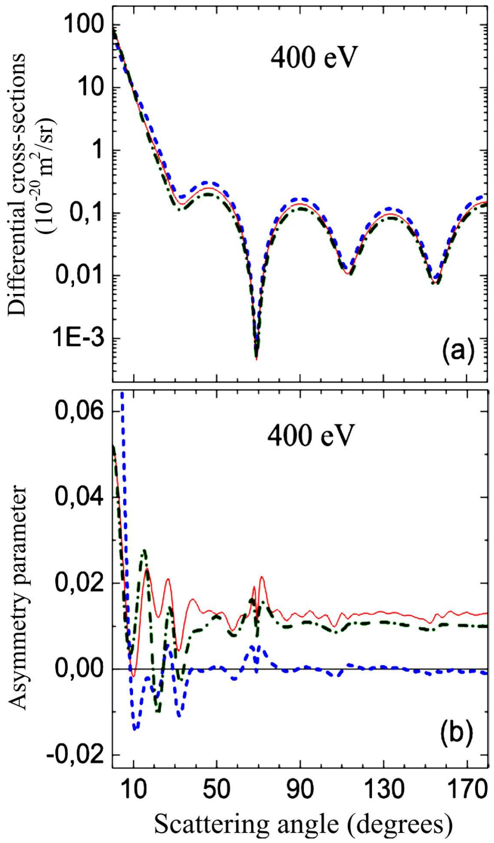

Fig. 3. (color on-line) Angular dependences of (a) the differential cross-sections (in units of [10^{-20} m^2 sr^{-1}]) and (b) the asymmetry parameter $A(E,\theta)$ for the elastic electron scattering by gold atoms at 400 eV: $V_{\rm opt}$ calculations (formula (1)) with the absorption potentials $VaMc_\lambda(r,E)$ (formula (6), solid curve) and $VaMc_\lambda(r,E)$ (dash-dotted curve); $V_{\rm R}$ calculations taking no absorption effects into account (formula (2), dashed curve)

400 eV. As the collision energy increases, the absolute value of asymmetry gradually decreases.

The process of electron scattering by a target atom with a half-filled s^1-subshell was considered in the spin-polarized approximation of the optical potential method. This approximation allowed the scattering of electrons with the spin directed parallel and antiparallel to the atom one to be described. Therefore, the interaction with gold atoms was considered in the approximations of two spin-orientation-dependent optical potentials. Namely, such scattering potentials as the exchange, polarization, and absorption ones, which are important for studying the spin asymmetry, are spin-dependent. The analytical expressions for them are presented.

Atomic characteristics needed for the determination of components of optical potentials are calculated self-consistently in the scalar-relativistic approximation and the local spin density approximation of the density functional theory. Analytical expressions are presented for the static potential, the total and spin electron densities, and the valence 6s-orbital, and the corresponding approximation parameters are determined.

Calculations are carried out with (in the approximation of complex-valued optical potential) and without (in the approximation of the parameter-free real-valued part of the optical potential) the absorption effects. The influence of absorption effects taken into account on the behavior of the angular asymmetry dependence is qualitatively and quantitatively considerable within the whole interval of collision energies. Moreover, even at 400 eV and scattering angles of 10–50°, the asymmetry is sensitive to the choice of absorption potential.

The researches fulfilled demonstrate a rather substantial influence of the spin dependence of the polarization interaction on the angular behavior of the asymmetry. This qualitative and quantitative influence reveals itself in the whole angle interval (0–180°) at low collision energies ($\leq$ 5 eV). As the energy increases, this interval gets narrower to 0–50° at 200 eV. The angle position of the high-angle peculiarity, which starts to affect the asymmetry at an angle of 142° for an energy of 60 eV, shifts to an angle of 86° for 200 eV. In so doing, it manifests itself as a maximum and a minimum–maximum. In the vicinity of this specific feature, the influence of spin dependences of the absorption and the exchange and polarization interactions is rather important.

The results of calculations of the asymmetry parameter, which were obtained in different optical potential approximations, show that this characteristic of scattering can serve as a sensitive test to the choice of experimental techniques and theoretical methods.

APPENDIX A. Analytical expressions and parameter values for the static potential $V_{\rm st}(r)$, the total, $\rho(r)$, and spin, $\rho_{\rm sp}(r)$, electron densities in a gold atom

The static potential $V_{\rm st}(r)$ and the electron densities $\rho(r)$ and $\rho_{\rm sp}(r)$ are calculated with the help of the following analytical expressions similar to those in work [19]:

$$V_{\rm st}(r) = -\frac{Z}{r}[\sum_{i=1}^{n} A_i \exp(-B_i r) + r\sum_{j=1}^{m} C_j \exp(-D_j r)], \qquad (A.1)$$

$$\rho_{sp}(r) = \frac{N_{sp}}{4\pi r}[\sum_{i=1}^{n} A_i B_i^2 \exp(-B_i r)+$$

$$+\sum_{j=1}^{m} C_j D_j (D_j r - 2)\exp(-D_j r)], \qquad (A.2)$$

where Z is the charge of a target atom. In Eq. (A.1), the number of terms $n = 5$ in the first sum, and $m = 5$ in the second. The parameters A_i, B_i, C_i, and D_i are as follows. The parameters $A_1 = 0.1989$, $A_2 = 0.1823$, $A_3 = -14.9053$, $A_4 = -0.00596$, and $A_5 = 1 - A_1 - A_2 - A_3 - A_4$ are dimensionless. The parameters $B_1 = 2.64$, $B_2 = 1.52$, $B_3 = 48.13$, $B_4 = 296$, $B_5 = 6.3112$, $C_1 = -22.022$, $C_2 = -317.41$, $C_3 = -163.33$, $C_4 = -71.104$, $C_5 = -54.129$, $D_1 = 66.016$, $D_2 = 35.87$, $D_3 = 18.974$, $D_4 = 12.544$, and $D_5 = 7.764$ are measured in units of a_0^{-1}, a_0 being the first Bohr radius of a hydrogen atom.

For the calculation of the total electron density $\rho(r)$, expression (A.1) is used, in which $n = 5$ and $m = 5$, $N_{sp} = Z$, and the parameters A_i, B_i, C_i, and D_i have the same values as indicated above.

For the calculation of $\rho_\uparrow(r)$ and $\rho_\downarrow(r)$ in expression (A.2), the number of terms $n = 4$ in the first sum and $m = 5$ in the second. For $\rho_\uparrow(r)$, the number of electrons with spin up in gold atom $N_\uparrow = 40$; the parameters $A_1 = 0.26002$, $A_2 = -14.0214$, $A_3 = -0.00684$, and $A_4 = 14.769$ are dimensionless; the parameters $B_1 = 1.487$, $B_2 = 48.179$, $B_3 = 279.6$, $B_4 = 6.1463$, $C_1 = -19.772$, $C_2 = -299.13$, $C_3 = -145.53$, $C_4 = -73.954$, $C_5 = -55.479$, $D_1 = 67.627$, $D_2 = 35.986$, $D_3 = 19.255$, $D_4 = 13.089$, and $D_5 = 7.7651$ are measured in units of a_0^{-1}.

For $\rho_\downarrow(r)$, the number of electrons with spin down in a gold atom $N_\downarrow = 39$; the parameters $A_1 = 0.26431$, $A_2 = -14.189$, $A_3 = -0.00815$, and $A_4 = 14.933$ are dimensionless; the parameters $B_1 = 1.87$, $B_2 = 46.111$, $B_3 = 267.8$, $B_4 = 5.4371$, $C_1 = -13.506$, $C_2 = -292.07$, $C_3 = -172.95$, $C_4 = -62.015$, $C_5 = -41.988$, $D_1 = 72.742$, $D_2 = 34.964$, $D_3 = 17.834$, $D_4 = 10.321$, and $D_5 = 6.695$ are measured in units of a_0^{-1}.

APPENDIX B. Auxiliary expression for the polarization potential (5)

In the nonrelativistic approximation, the correlation energy density is written down in the form (in a.u.) [30, 31]

$$\varepsilon_c(r_s,\zeta) = \varepsilon_c^P(r_s) + \Delta\varepsilon_c(r_s,\zeta), \tag{B.1}$$

where $\varepsilon_c^P(r_s) = \varepsilon_c(r_s,0)$ (see also expression (24) in work [18]) and $\Delta\varepsilon_c(r_s,0) = 0$. For the spin-dependent part of $\Delta\varepsilon_c(r_s,\zeta)$, the following expression was used [30, 31]:

$$\Delta\varepsilon_c(r_s,\zeta) = \alpha_c(r_s)\frac{f(\zeta)}{f''(0)}[1 + \beta_c(r_s)\zeta^4]. \tag{B.2}$$

where

$$\begin{gathered}\beta_c(r_s) = f''(0)\,\Delta\varepsilon_c(r_s,1)/\alpha_c(r_s) - 1,\\ \Delta\varepsilon_c(r_s,1) = \varepsilon_c^F(r_s) - \varepsilon_c^P(r_s),\\ \varepsilon_c^F(r_s) = \varepsilon_c(r_s,1),\\ f(\zeta) = \frac{(1+\zeta)^{4/3} + (1-\zeta)^{4/3} - 2}{2(2^{1/3}-1)}, \\ f'(\zeta) = \frac{2[(1+\zeta)^{1/3} - (1-\zeta)^{1/3}]}{3(2^{1/3}-1)},\\ f''(\zeta) = \frac{2[(1+\zeta)^{-2/3} + (1-\zeta)^{-2/3}]}{9(2^{1/3}-1)},\\ f''(0) = \frac{4}{9(2^{1/3}-1)},\\ f(0) = 0, \qquad f(1) = 1.\end{gathered} \tag{B.3}$$

The correlation part $\alpha_c(r_s)$ of the spin displacement functions in expression (B.2) and the densities $\varepsilon_c^P(r_s)$ and $\varepsilon_c^F(r_s)$ in formulas (B.1) and (B.3) were approximated by the same expression [32]

$$g(x(r_s)) = A\left\{\ln\frac{x^2}{X(x)} + \frac{2B}{Q}\arctan\frac{Q}{2x+B} - \right.$$
$$\left. -\frac{Bx_0}{X(x_0)}\left[\ln\frac{(x-x_0)^2}{X(x)} + \frac{2(B+2x_0)}{Q}\arctan\frac{Q}{2x+B}\right]\right\}, \tag{B.4}$$

where $x = (r_s)^{1/2}$, $X = x^2 + Bx + C$, and $Q = [4C - B^2]^{1/2}$. The approximation coefficients A, B, C, and x_0 in expression (B.4) are as follows: for $\alpha_c(r_s)$, $A = -0.01688685$, $B = 1.13107$, $C = 13.0045$, $x_0 = -0.00475840$; for $\varepsilon_c^P(r_s)$, $A = 0.0310907$, $B = 3.72744$, $C = 12.9352$, $x_0 = -0.10498$; for $\varepsilon_c^F(r_s)$, $A = 0.01554535$, $B = 7.06042$, $C = 18.0578$, $x_0 = -0.32500$.

The derivatives with respect to r_s in Eq. (5) are equal to

$$\frac{\partial\varepsilon_c}{\partial r_s} = \frac{1}{2\sqrt{r_s}}\frac{\partial\varepsilon_c}{\partial x},$$

$$\frac{\partial\varepsilon_c}{\partial x} = [1 - f(\zeta)\zeta^4]\frac{d\varepsilon_c^P}{dx} + f(\zeta)\zeta^4\frac{d\varepsilon_c^F}{dx} + \frac{f(\zeta)}{f''(0)}(1-\zeta^4)\frac{\partial\alpha_c}{\partial x}. \tag{B.5}$$

The derivatives $\frac{d\varepsilon_c^P}{dx}$, $\frac{d\varepsilon_c^F}{dx}$, and $\frac{\partial\alpha_c}{\partial x}$ in formulas (B.5) were approximated by the same expression [32]

$$\frac{dg}{dx} = A\left\{\frac{2}{x} - \frac{(2x+B)}{X(x)}\frac{(C+x_0^2)}{X(x_0)} - \frac{2Bx_0}{(x-x_0)X(x_0)} - \right.$$
$$\left. -\frac{B}{X(x)}\frac{(C-x_0^2)}{X(x_0)}\right\}. \tag{B.6}$$

The derivative $\frac{\partial\varepsilon_c}{\partial\zeta}$ in expression (5) is determined by the formula

$$\frac{\partial\varepsilon_c}{\partial\zeta} = \left[\varepsilon_c^F(x) - \varepsilon_c^P(x) - \frac{\alpha_c(x)}{f''(0)}\right]\times$$
$$\times\left[4f(\zeta) + f'(\zeta)\cdot\zeta\right]\zeta^3 + \alpha_c(x)\frac{f'(\zeta)}{f''(0)}. \tag{B.7}$$

APPENDIX C. Analytical expressions and parameter values for the $6s$-valence electron density $\rho_{6s}(r)$ in a gold atom

The analytical expression for the electron density of the valence $6s$-subshell looks like

$$\rho_{6s}(r) = \varphi_{6s}^2(r), \tag{C.1}$$

where

$$\varphi_{6s}(r) = \sum_{i=1}^{5} K_i r^{M_i}\exp(-N_i r). \tag{C.2}$$

is a Slater electron orbital (see [22] and references therein). The parameter values in Eq. (C.2) are as follows: $K_1 = 27.095$, $K_2 = -61.702$, $K_3 = 4.112$, $K_4 = -12.582$, $K_5 = -2.3943$, $M_1 = -0.4595$, $M_2 = 0.09875$, $M_3 = -1.0185$, $M_4 = -0.6954$, $M_5 = -1.0648$, $N_1 = 8.979$, $N_2 = 19.9103$, $N_3 = 1.1216$, $N_4 = 5.1693$, and $N_5 = 0.66234$. The parameters M_i are dimensionless, and the parameters N_i are expressed in units of a_0^{-1}. The dimension of the parameters K_i is defined by the normalization of the density ρ_{6s}.

1. J.C. Slater, *The Self-Consistent Field for Molecules and Solids* (McGraw-Hill, New York, 1974).
2. *Theory of the Inhomogeneous Electron Gas*, edited by S. Lundqvist and N.H. March (Plenum Press, New York, 1983).
3. M. Zubek, A. Danjo, and G.C. King, J. Phys. B **28**, 4117 (1995).
4. O. Berger and J. Kessler, J. Phys. B **19**, 3539 (1986).
5. S. Holst, W. Legler, R. Newjoto, and J. Peters, J. Phys. B **23**, 2977 (1990).
6. J.M. Schroeer, D.H. Gündüz, and S. Livingston, J. Chem. Phys. **58**, 5135 (1973).
7. H. Mahide, M. Nagasu, H. Takahashi, and T. Nagata, in *Proceedings of the 24th International Conference on Photonic, Electronic and Atomic Collisions*, edited by F.D. Colavecchia *et al.*, (Rosario, Argentina, 2005), p. Mo039.
8. J.K. O'Connell and N.F. Lane, Phys. Rev. A **27**, 1893 (1983).
9. N.T. Padial and D.W. Norcross, Phys. Rev. A **29**, 1742 (1984).
10. E.Yu. Remeta and V.I. Kelemen, J. Phys. B **43**, 045202 (2010).
11. J.B. Furness and I.E. McCarthy, J. Phys. B **6**, 2280 (1973).
12. I. McCarthy, C. Noble, B. Phillips, and A.Turnbull, Phys. Rev. A **15**, 2173 (1977).
13. G. Staszewska, D.W. Schwenke, and D.G. Truhlar, Phys. Rev. A **29**, 3078 (1984).
14. S.D. Tošić, M.S. Rabasović, D. Šević, V. Pejćev, D.M. Filipović, L. Sharma, A.N. Tripathi, R. Srivastava, and B.P. Marinković, Phys. Rev. A **77**, 012725 (2008).
15. M.S. Rabasović, V.I. Kelemen, S.D. Tošić, D. Šević, M.M. Dovhanych, V. Pejćev, D.M. Filipović, E.Yu. Remeta, and B.P. Marinković, Phys. Rev. A **77**, 062713 (2008).
16. V.I. Kelemen, M.M. Dovhanych, and E.Yu. Remeta, J. Phys. B **41**, 035204 (2008).
17. V.I. Kelemen, M.M. Dovhanych, and E.Yu. Remeta, J. Phys. B **41**, 125202 (2008).
18. V. Kelemen, E. Remeta, and E. Sabad, J. Phys. B **28**, 1527 (1995).
19. T.G. Strand and R.A. Bonham, J. Chem. Phys. **40**, 1686 (1964).
20. V.I. Kelemen, Tech. Phys. **47**, No. 9, 1083 (2002).
21. V.I. Kelemen, E.P. Sabad, and M.M. Dovhanych, Ukr. Fiz. Zh. **34**, 345 (1989).
22. A.A. Radtsig and B.M. Smirnov, *Reference Data on Atoms, Molecules, and Ions* (Springer, Berlin, 1986).
23. A. Zangwill and P. Soven, Phys. Rev. A **21**, 1561 (1980).
24. S.D. Tošić, V.I. Kelemen, D. Šević, V. Pejćev, D.M. Filipović, E.Yu. Remeta, and B.P. Marinković, Nucl. Instrum. Methods B **267**, 283 (2009).
25. F. Calogero, *Variable Phase Approach to Potential Scattering* (Academic Press, New York, 1967).
26. V.V. Babikov, *Phase Function Method in Quantum Mechanics* (Nauka, Moscow, 1988) (in Russian).
27. J. Kessler, Adv. At. Mol. Opt. Phys. **27**, 81 (1991).
28. R.S. Freund, R.C. Wetzel, R.J. Shul, and T.R. Hayes, Phys. Rev. A **41**, 3575 (1990).
29. W. Lotz, Z. Physik **232**, 101 (1970).
30. S.H. Vosko, L. Wilk, and M. Nusair, Can. J. Phys. **58**, 1200 (1980).
31. D.M. Ceperly and B.J. Alder, Phys. Rev. Lett. **45**, 566 (1980).
32. G.S. Painter, Phys. Rev. B **24**, 4264 (1981).

Received 17.02.10.
Translated from Ukrainian by O.I. Voitenko

АСИМЕТРІЯ У ПРУЖНОМУ РОЗСІЮВАННІ ЕЛЕКТРОНІВ АТОМАМИ ЗОЛОТА

В.І. Келемен, М.М. Довганич, Є.Ю. Ремета

Резюме

У спін-поляризованному наближенні методу оптичного потенціалу (ОП) досліджено кутову залежність параметра спінової обмінної асиметрії у пружному розсіюванні електронів на атомах золота в діапазоні енергій зіткнення 0,2–400 еВ. Розрахунки проведено як у наближенні безпараметричної дійсної частини ОП, так і з використанням комплексного ОП для врахування ефектів поглинання. У ролі уявної частини ОП використано два типи потенціалу поглинання. Систематичні розрахунки асиметрії проведено з використанням емпіричного потенціалу поглинання. Енергетичну залежність параметра в цьому потенціалі знайдено з використанням неемпіричного потенціалу поглинання в наближенні квазівільного розсіювання електронів. Показано, що поведінка кутової залежності параметра асиметрії в широкому інтервалі енергії визначається спіновою залежністю не тільки обмінної, але і поляризаційної взаємодії електрона з атомом. Відзначено великий вплив ефектів поглинання на поведінку параметра асиметрії. Показано, що навіть для енергій у декілька сот електрон-вольтів параметр асиметрії при малих кутах залежить від вибору того чи іншого потенціалу поглинання.